Electronic Supplementary Material (ESI) for Polymer Chemistry.

Sustainable Near UV-curable Acrylates Based on Natural Phenolics for Stereolithography 3D Printing

Rui Ding[†], Yuyang Du[‡], Rebecca Goncalves[§], Lorraine Francis[‡], Theresa M. Reineke*[,†]

[†]Department of Chemistry and Center for Sustainable Polymers, University of Minnesota, Minneapolis

[‡]Department of Chemical Engineering and Materials Science, University of Minnesota, Minneapolis

[§]Department of Chemistry, The College of New Jersey, New Jersey

Supplementary Information

Table of Contents

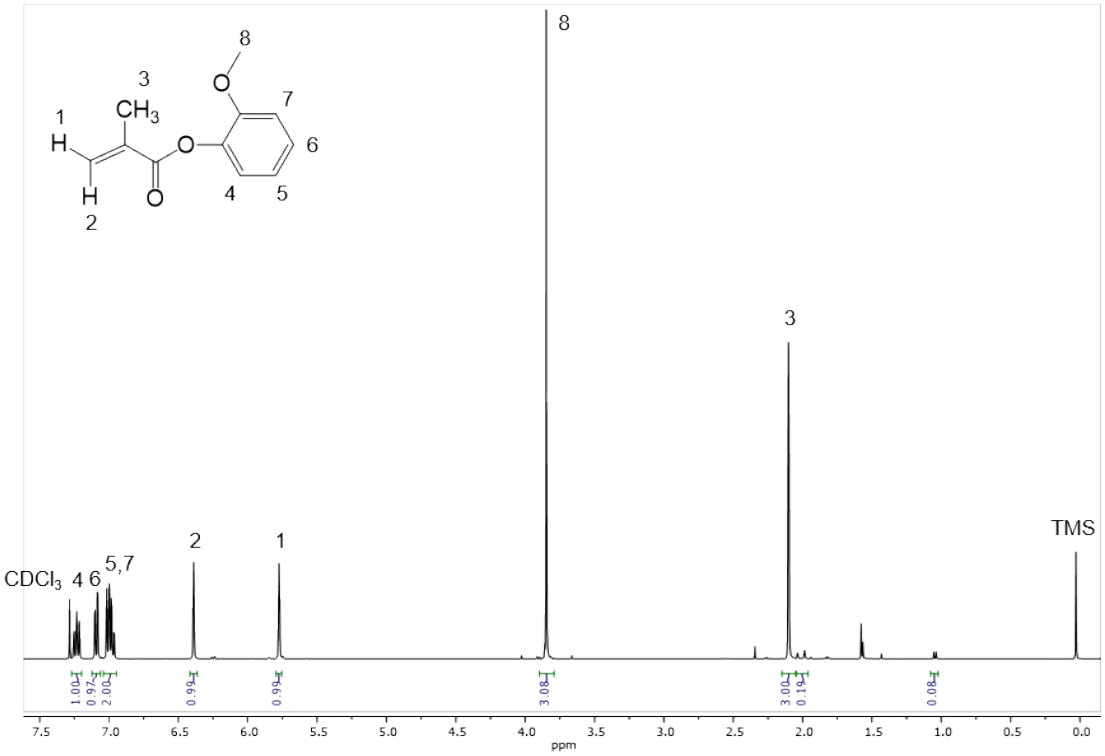

Figure S1. ^{1}H NMR spectrum of guaiacol methacrylate (**G**), in $CDCl_3$.

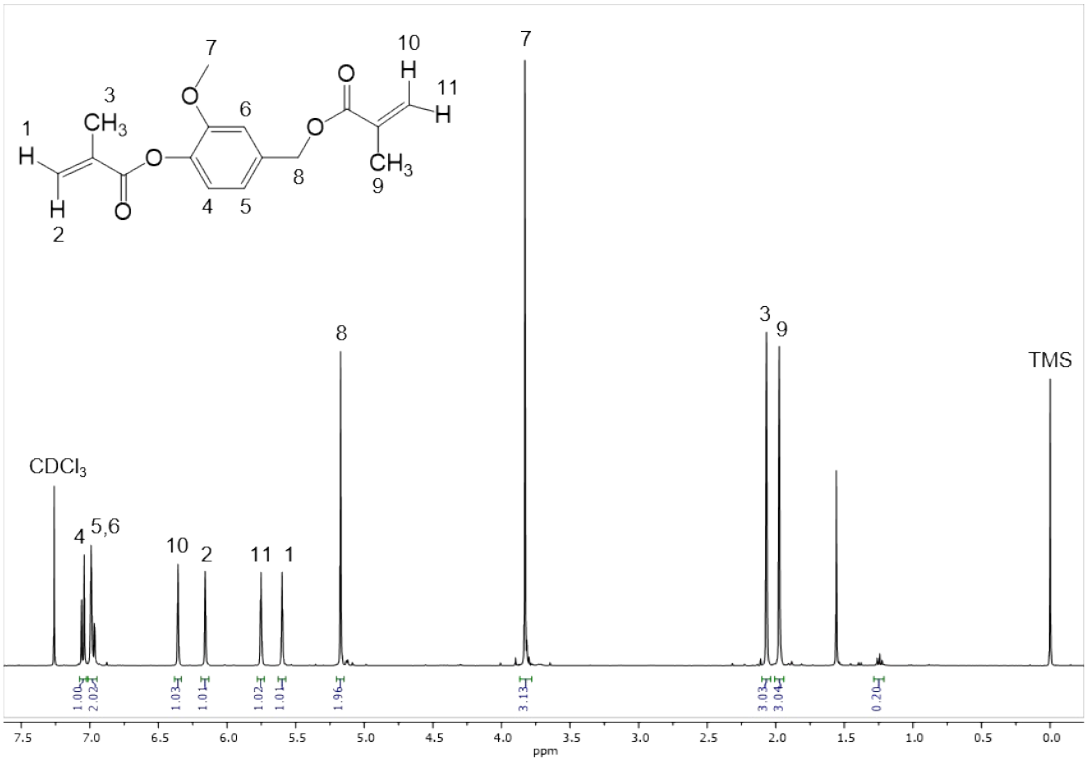

Figure S2. ^{1}H NMR spectrum of vanillyl alcohol methacrylate (**V**), in $CDCl_3$.

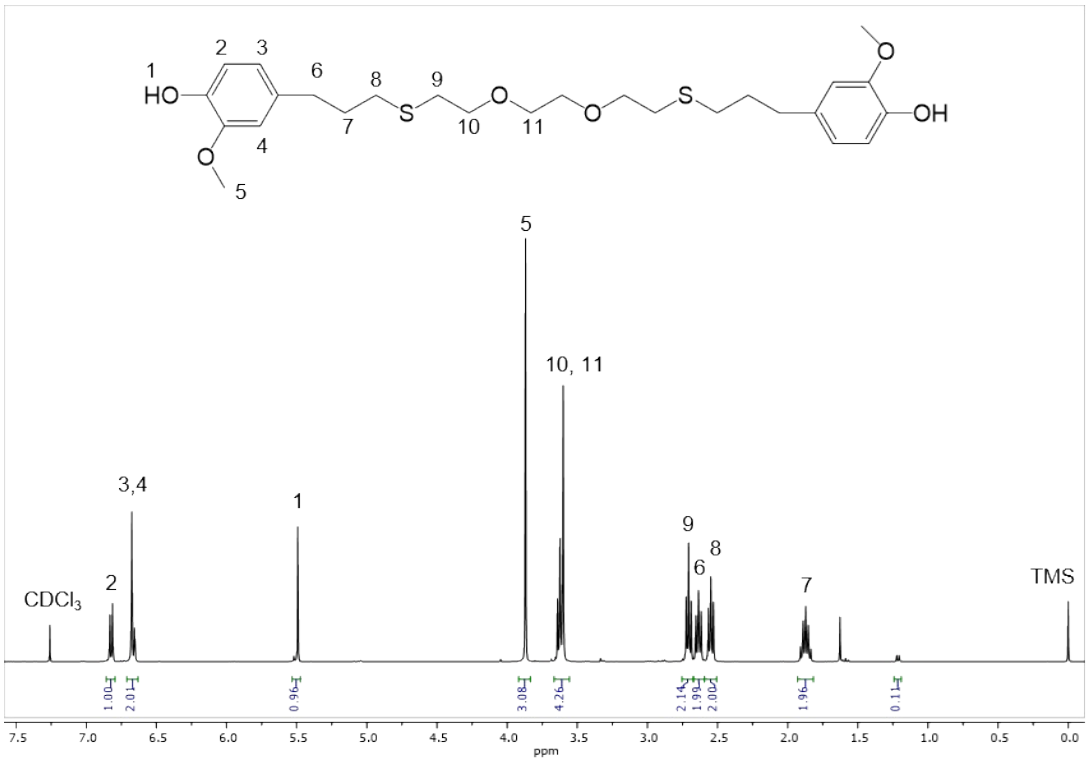

Figure S3. ^{1}H NMR spectrum of 3,6-dioxa-1,8-octanedithiol eugenol, in $CDCl_3$.

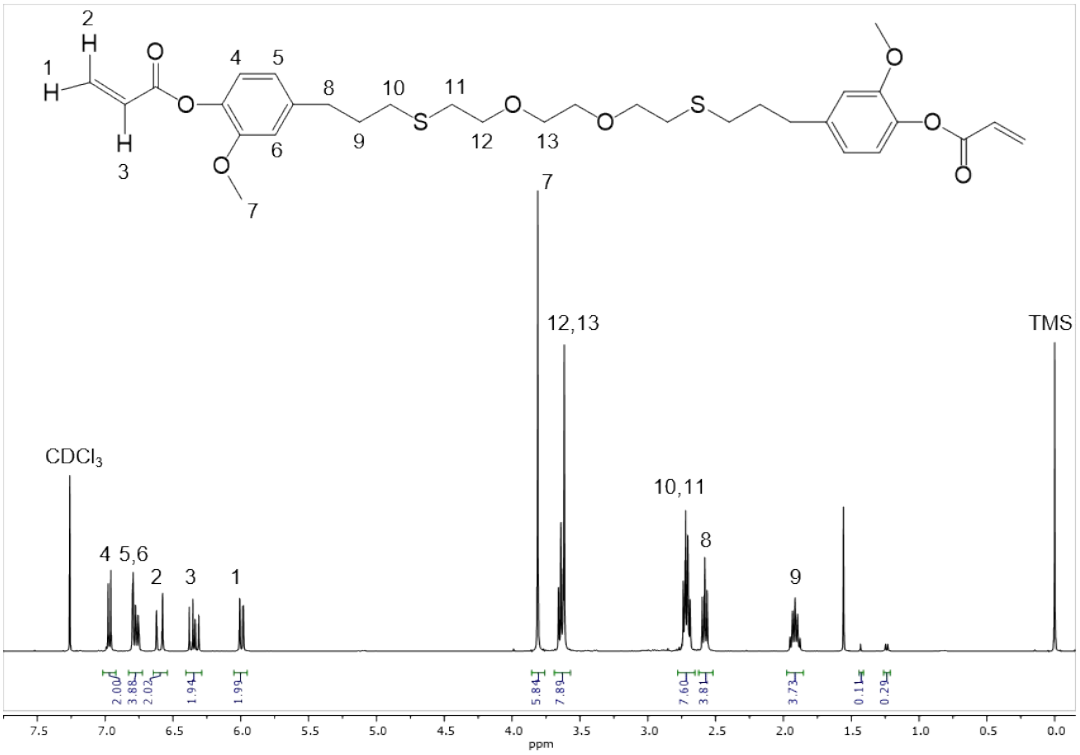

Figure S4. ^{1}H NMR spectrum of 3,6-dioxa-1,8-octanedithiol eugenol acrylate (**E**), in $CDCl_3$.

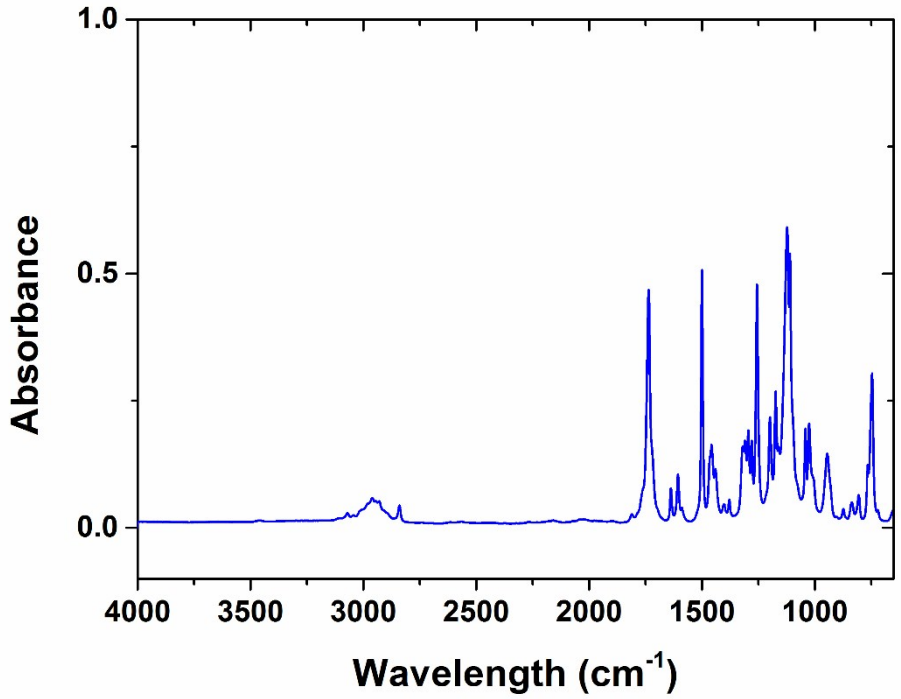

Figure S5. ATR-FTIR spectrum of guaiacol methacrylate (**G**). A droplet of liquid sample was spread on the ATR diamond crystal for measurement at room temperature.

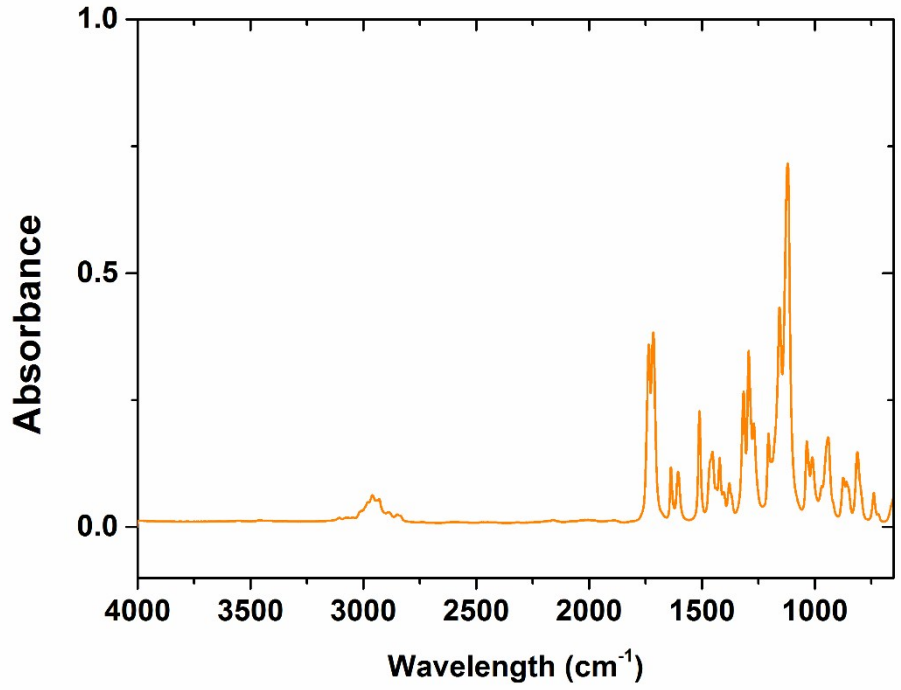

Figure S6. ATR-FTIR spectrum of vanillyl alcohol methacrylate (**V**). Sample was melted into a liquid and added as a droplet to the ATR diamond crystal for measurement at room temperature.

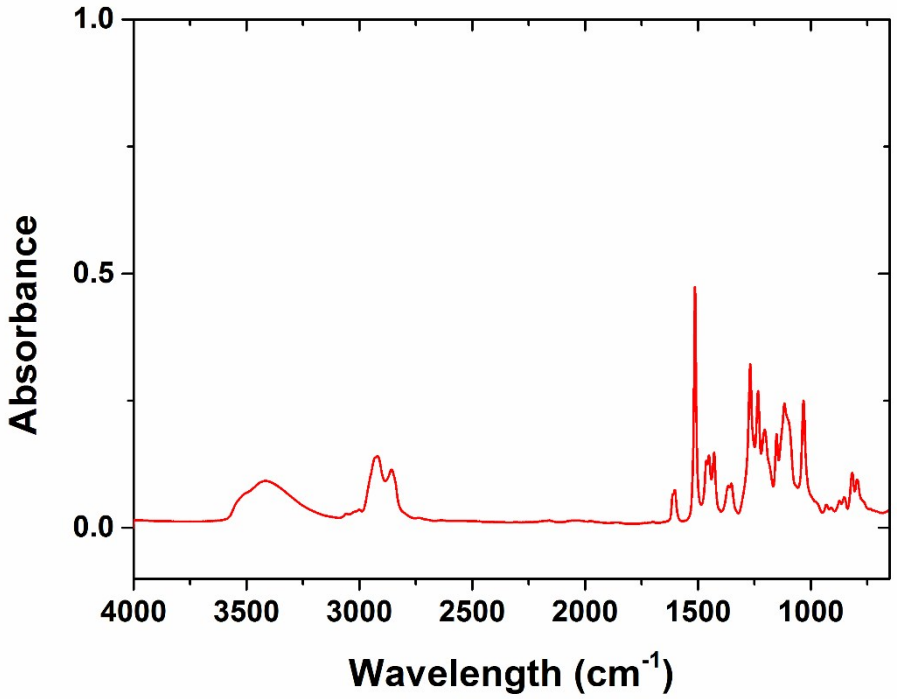

Figure S7. ATR-FTIR spectrum of 3,6-dioxa-1,8-octanedithiol eugenol. A droplet of liquid sample was spread on the ATR diamond crystal for measurement at room temperature.

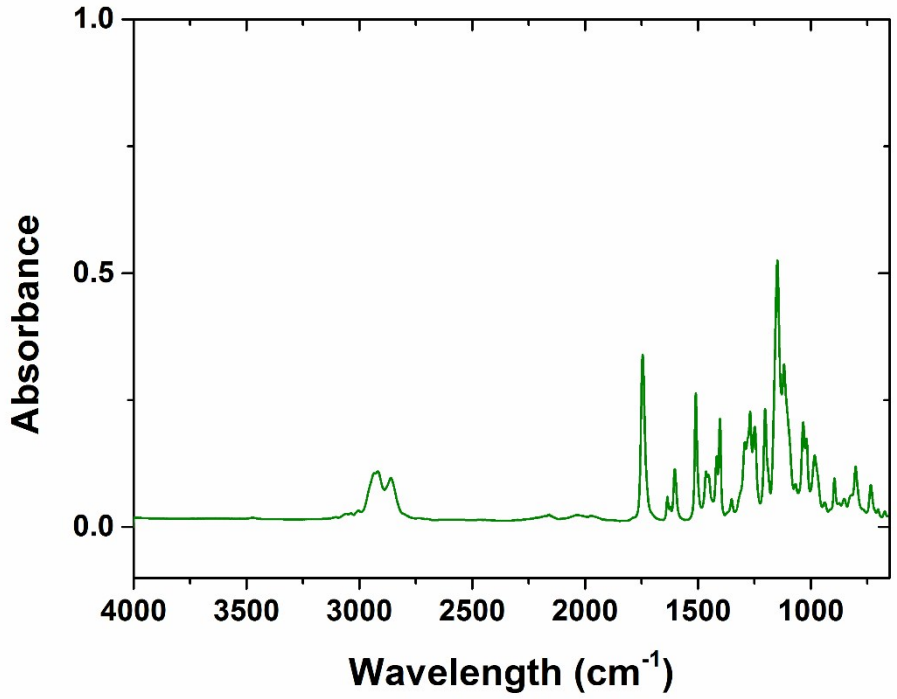

Figure S8. ATR-FTIR spectrum of 3,6-dioxa-1,8-octanedithiol eugenol acrylate (**E**). A droplet of liquid sample was spread on the ATR diamond crystal for measurement at room temperature.

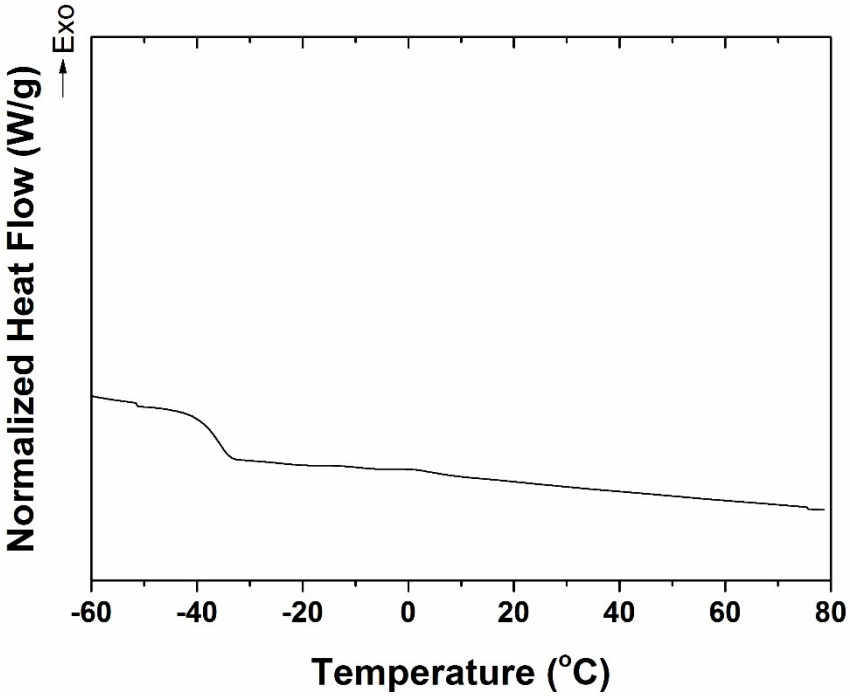

Figure S9. DSC thermogram of 3,6-dioxa-1,8-octanedithiol eugenol acrylate (**E**) at a heating rate of 10 °C/min.

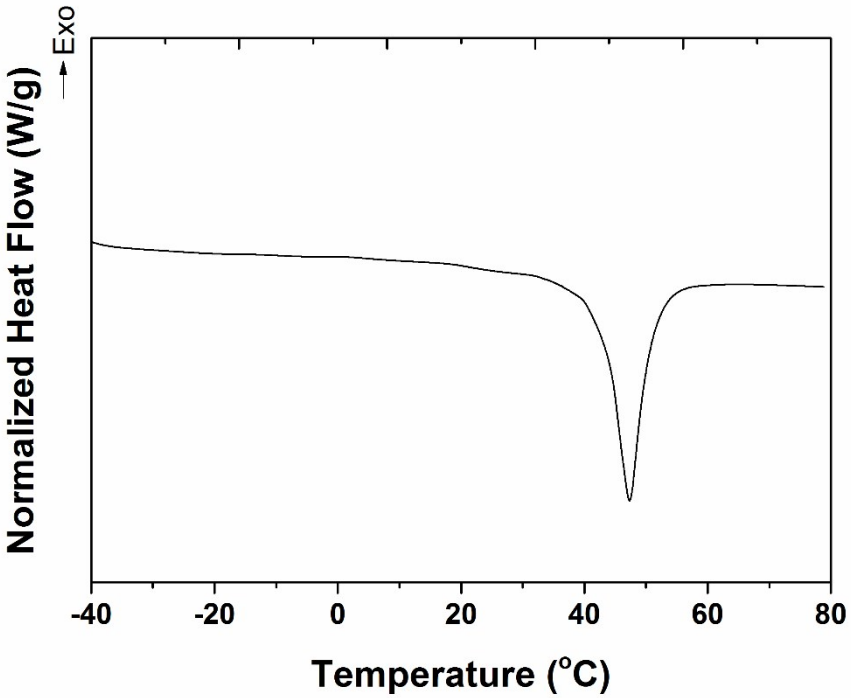

Figure S10. DSC thermogram of vanillyl alcohol methacrylate (**V**) at a heating rate of 10 °C/min.

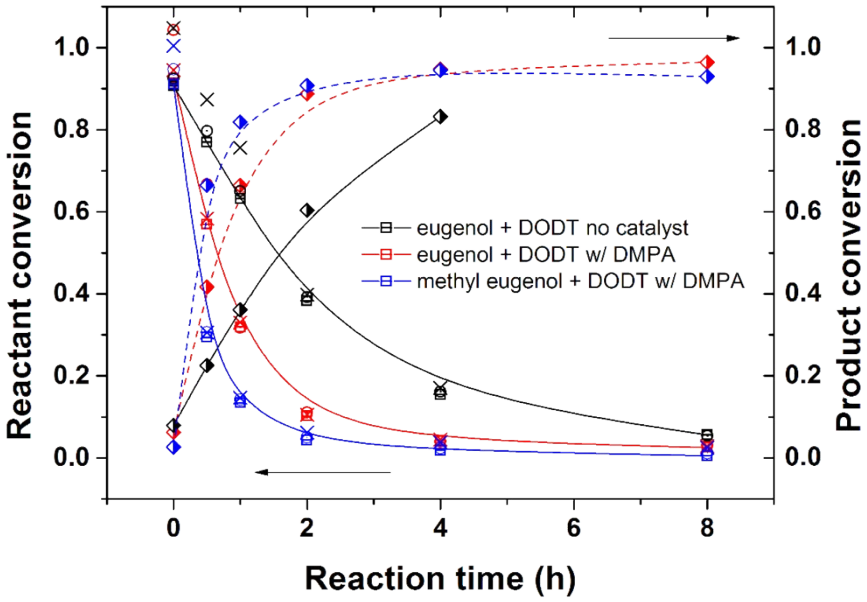

Figure S11. Reaction kinetic study of 3,6-dioxa-1,8-octanedithiol (DODT)-eugenol radical addition initiated by UV irradiation determined by ^{1}H NMR spectroscopy. Three reaction mixtures with a stoichiometric ratio (thiol: ene = 1:2) were compared: DODT + eugenol with no catalyst (black); DODT + eugenol with 0.5 wt.% 2,2-dimethoxy-2-phenylacetophenone (DMPA) as the catalyst; DODT + methyl eugenol with 0.5 wt% DMPA as the catalyst. The solid curves represent the consumption of reactants: (×) denotes the protons -CH_2-CH=C**H$_2$** at 5.03-5.09 ppm from eugenol; (□) denotes the protons -CH_2-C**H**=CH_2 at 5.89-5.99 ppm from eugenol; (○) denotes the protons -**SH** at 1.56-1.65 ppm from DODT. The dash curves represent the conversion of the thioether product: (◊) denotes the protons -C**H$_2$**-CH_2-S-$(CH_2)_2$-O- at 1.85-1.90 ppm from the thioether.

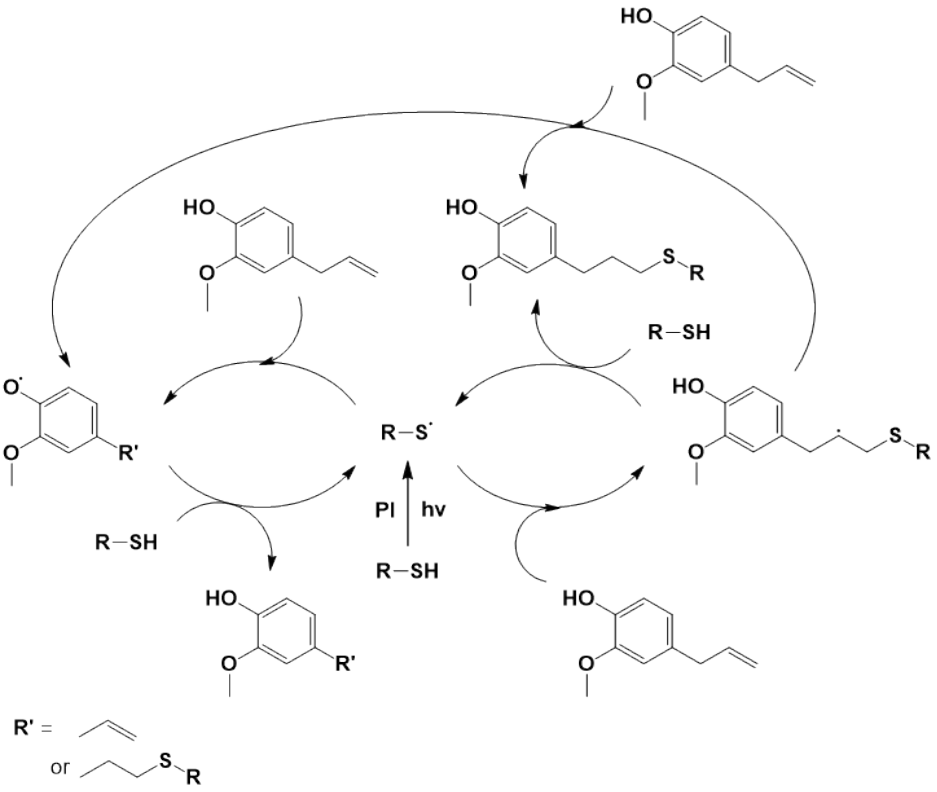

Figure S12. Proposed mechanism of radical addition between 3,6-dioxa-1,8-octanedithiol and eugenol. The phenolic hydroxyl group causes additional routes to transfer the thiyl and carbon radical that retard the thiol-ene reaction rate. The final product is only thioether.

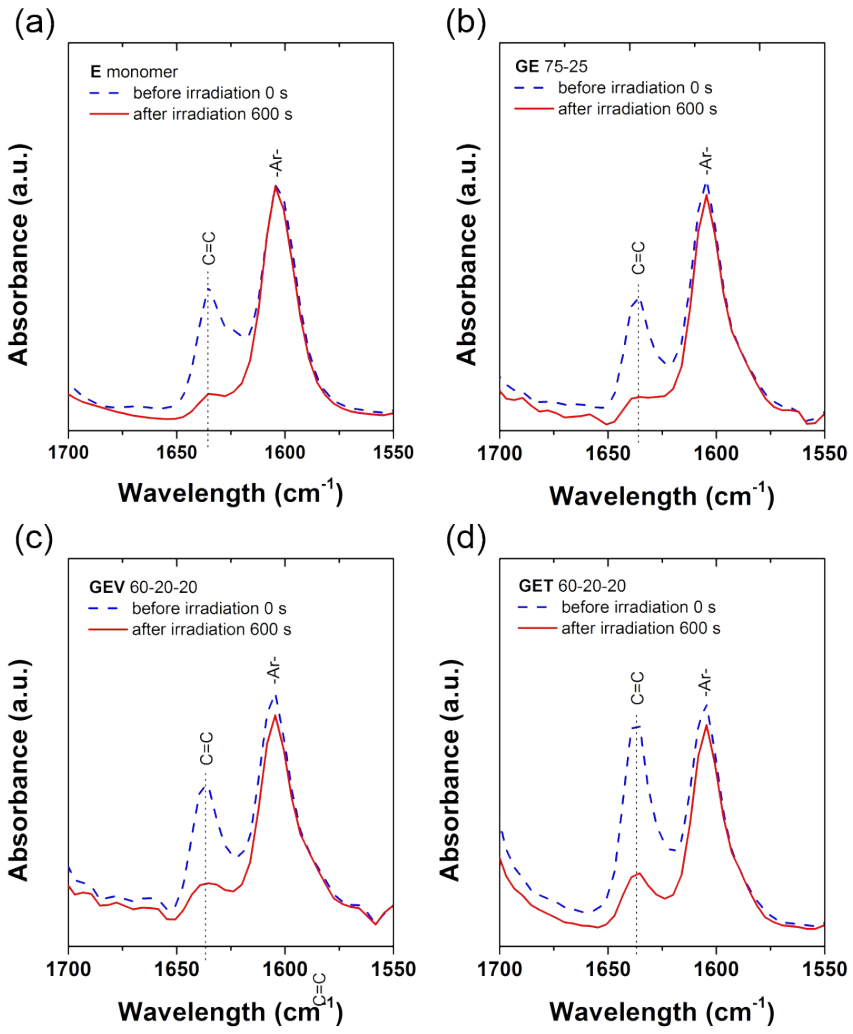

Figure S13. Magnified real-time FTIR spectra of different resin formulation examples before and after irradiation for 600 s: (a) **E**, (b) **GE** 75-25, (3) **GET** 60-20-20, (d) **GEV** 60-20-20. The peak at 1636 cm^{-1} is assigned to the (meth)acrylate C=C double bond absorption, which decrease as a function of irradiation time. The peak at 1604 cm^{-1} is assigned to the aromatic absorption, which remains constant with irradiation and thus used as reference peak for the calculating the conversion. The light intensity is 2 mW/cm^2.

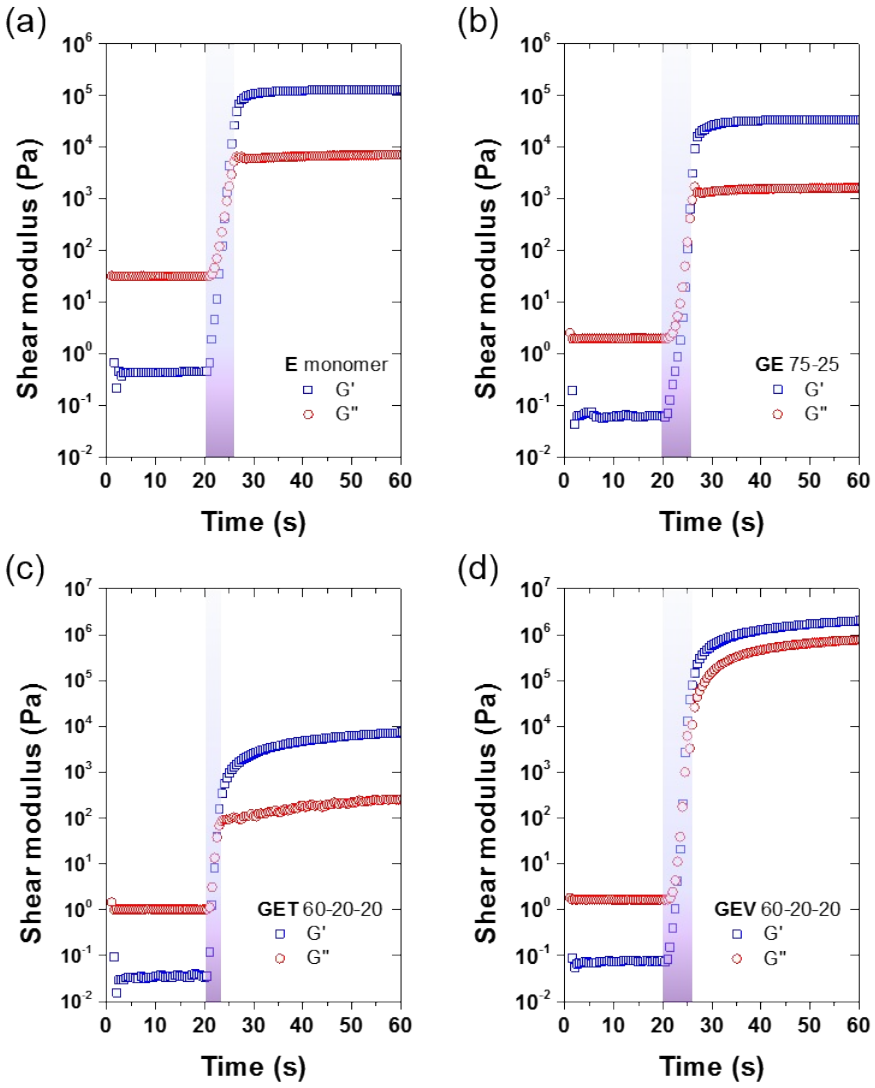

Figure S14. Photorheology of different resin formulation examples showing storage shear modulus and loss shear modulus as a function of time: (a) **E**, (b) **GE** 75-25, (3) **GET** 60-20-20, (d) **GEV** 60-20-20. The purple band indicates the duration of irradiation, which is triggered at 20 s after the rheology measurement started. The light intensity is 5 mW/cm^2.

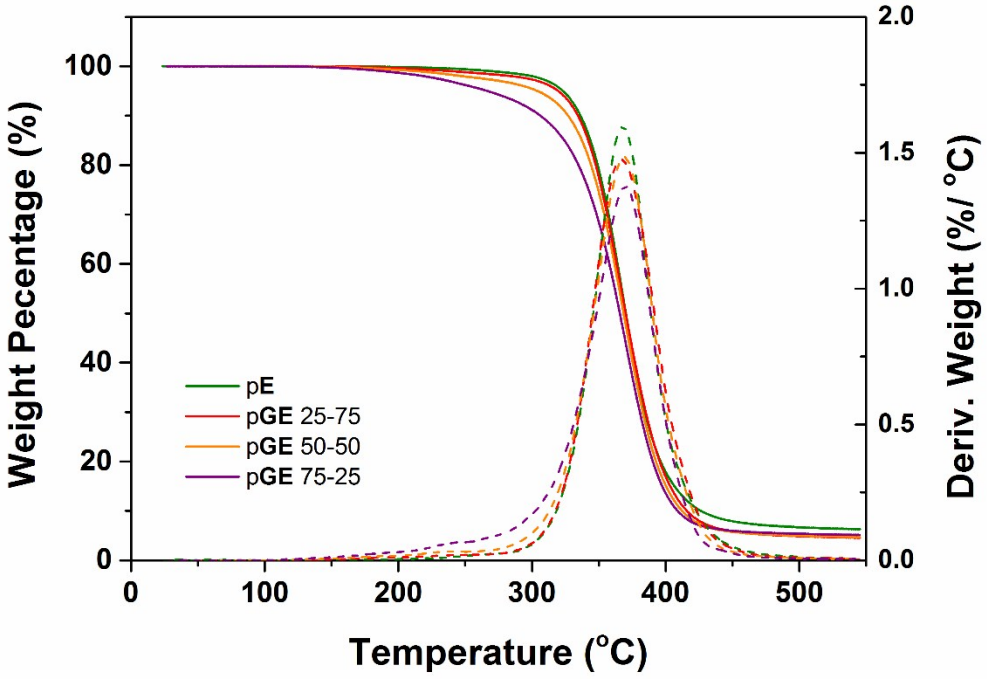

Figure S15. TGA of p**GE** binary polymers at different **G:E** ratios under a nitrogen atmosphere.

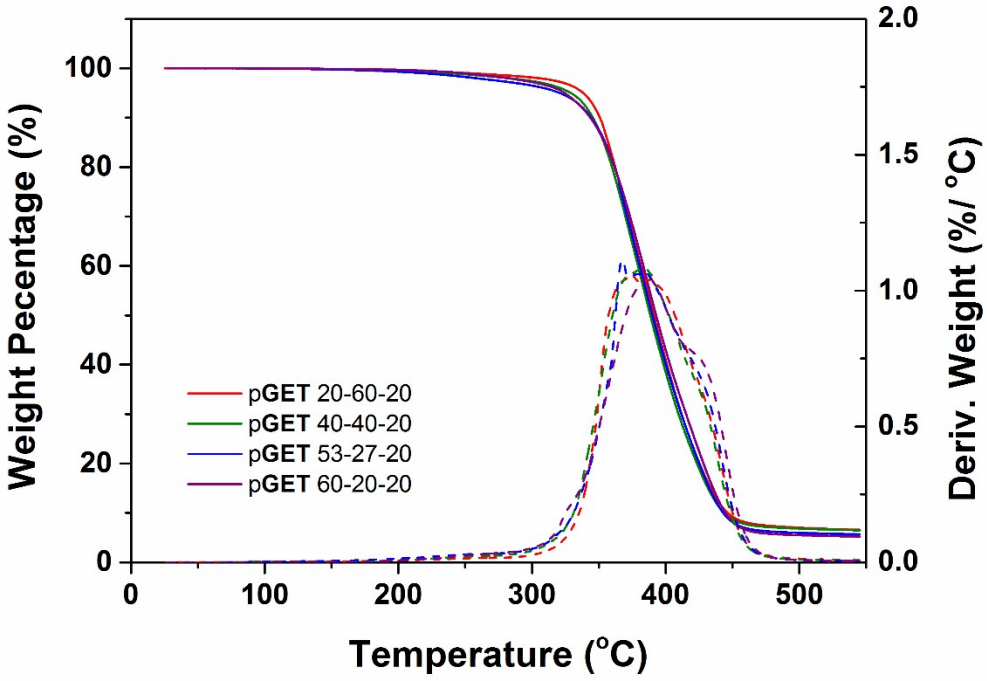

Figure S16. TGA of p**GET** terpolymers at different **G:E** ratios under a nitrogen atmosphere.

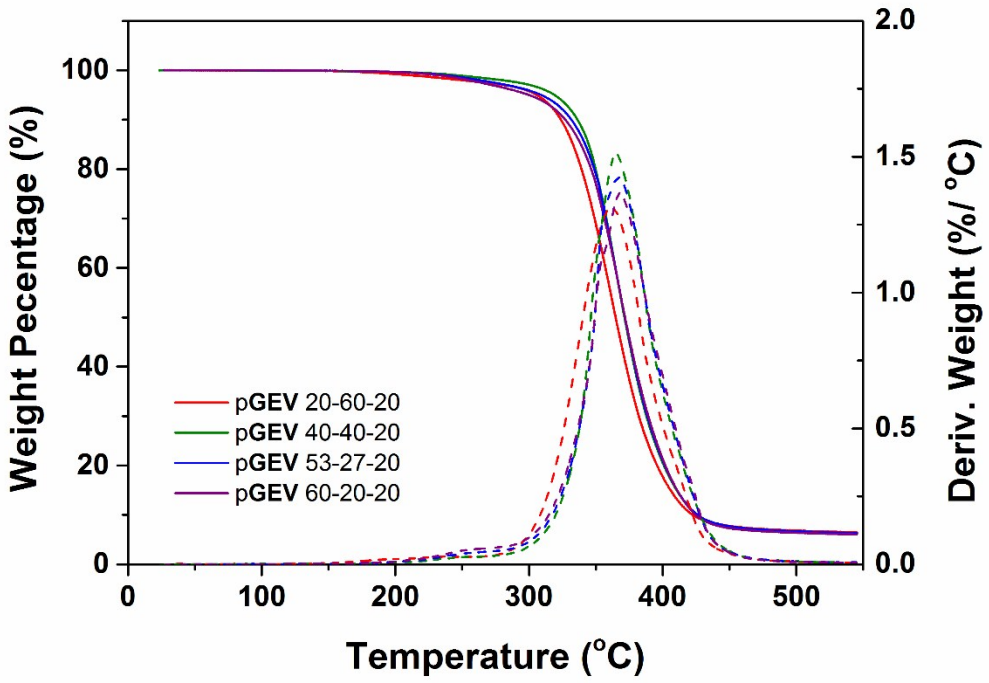

Figure S17. TGA of p**GEV** terpolymers at different **G:E** ratios under a nitrogen atmosphere.

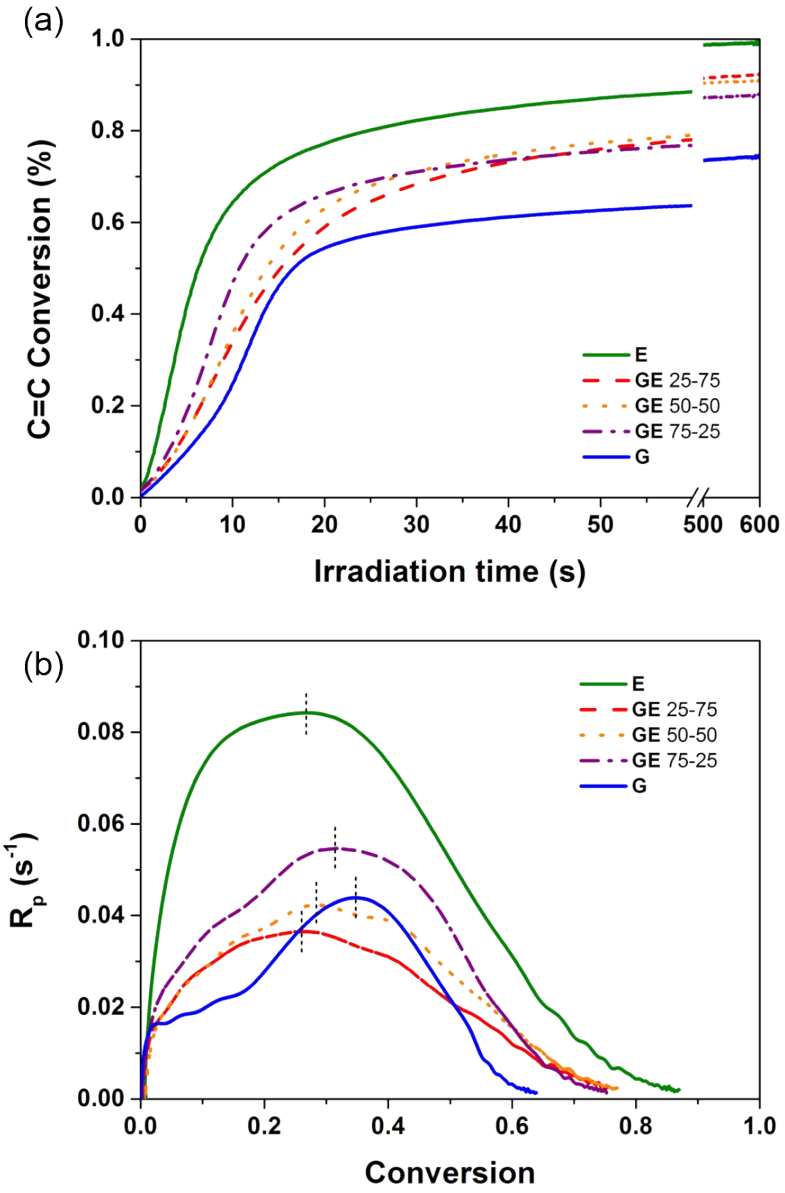

Figure S18. Photopolymerization kinetic profiles of **GE** binary polymers at different **G:E** ratios determined by real time-FTIR. (a) C=C conversion as a function of UV irradiation time (b) Polymerization rate as a function of monomer conversion at irradiation intensity of 2 mW/cm^2.

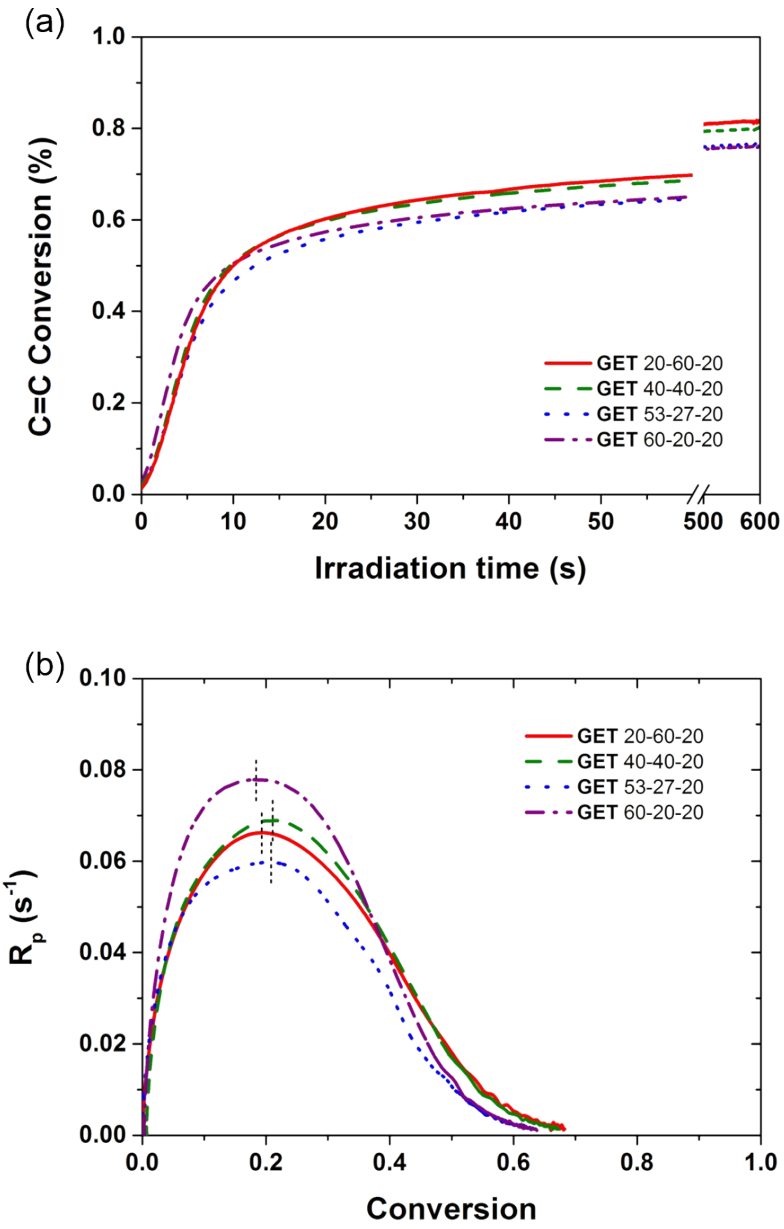

Figure S19. Photopolymerization kinetic profiles of **GET** ternary formulations at different **G:E** ratios determined by real time-FTIR. (a) C=C conversion as a function of UV irradiation time (b) Polymerization rate as a function of monomer conversion at irradiation intensity of 2 mW/cm^2.

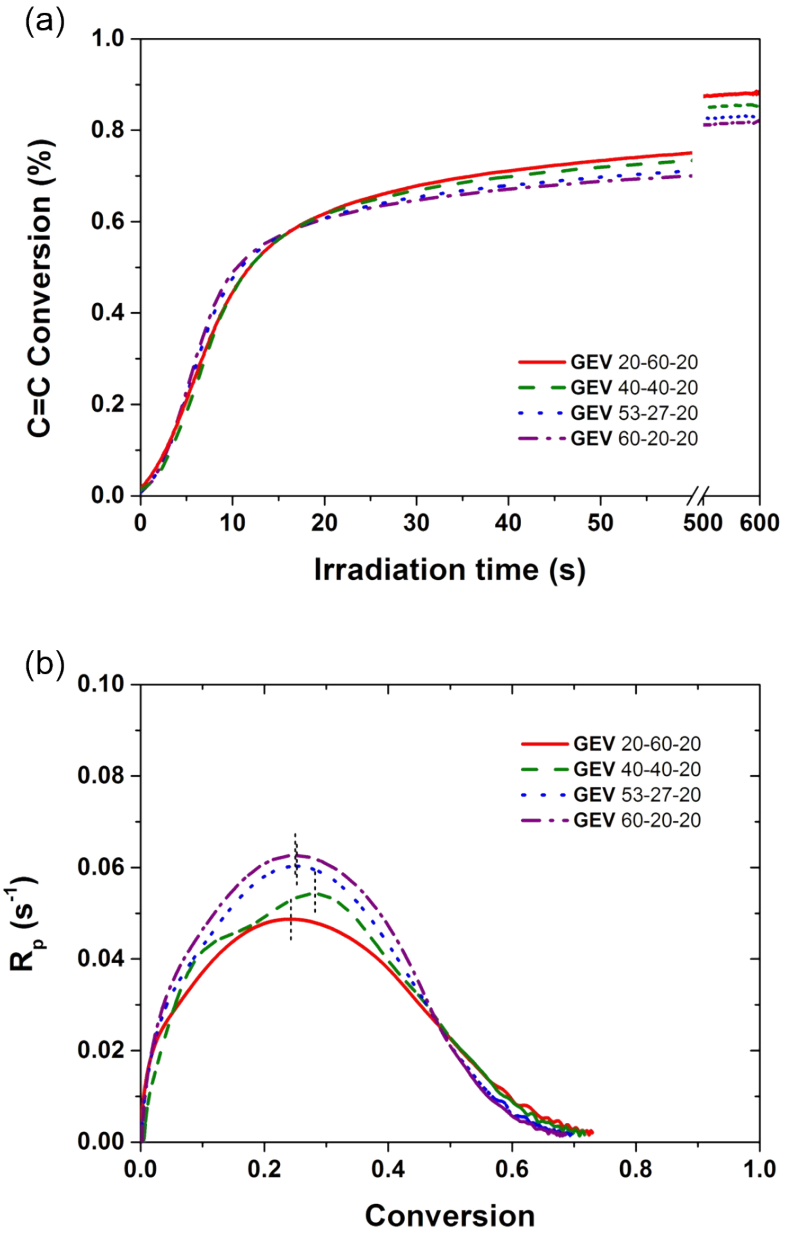

Figure S20. Photopolymerization kinetic profiles of **GEV** ternary formulations at different **G:E** ratios determined by real time-FTIR. (a) C=C conversion as a function of UV irradiation time (b) Polymerization rate as a function of monomer conversion at irradiation intensity of 2 mW/cm^2.

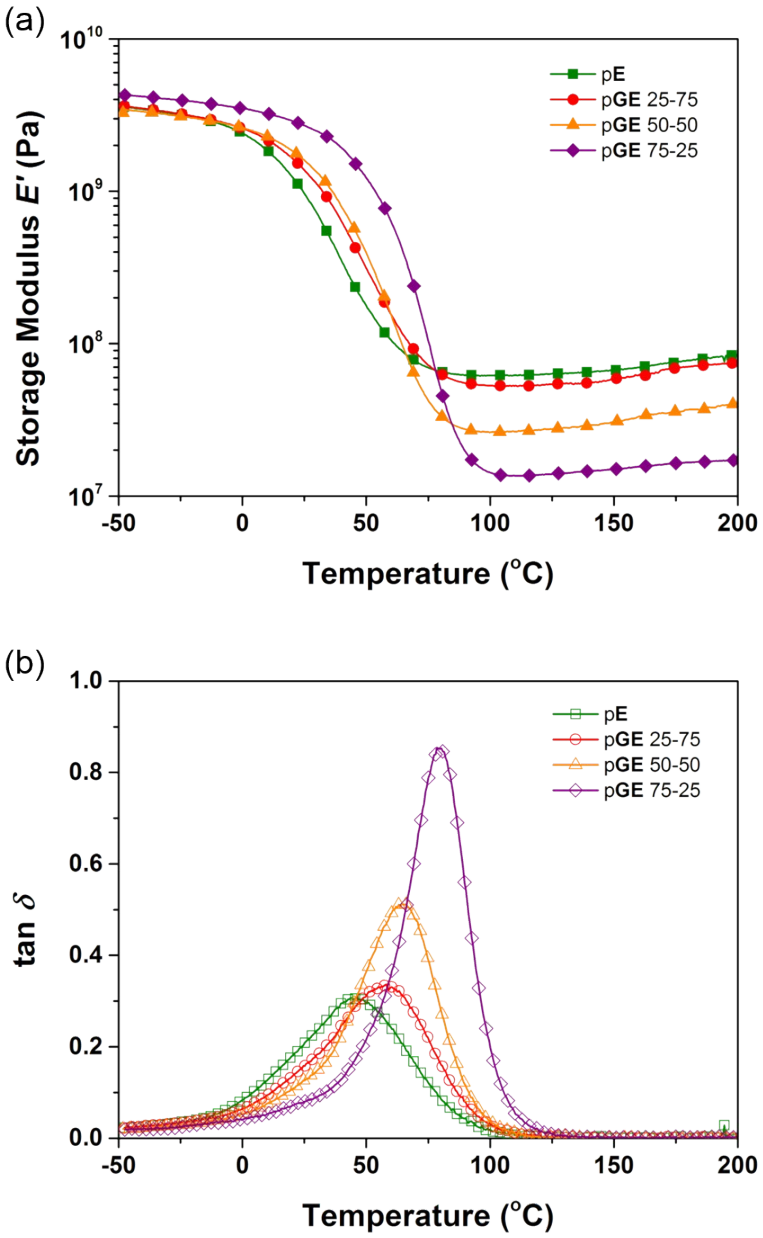

Figure S21. DMA of p**GE** binary polymers at different **G:E** ratios (a) storage modulus *E'* and (b) dissipation peak tan δ as a function of temperature.

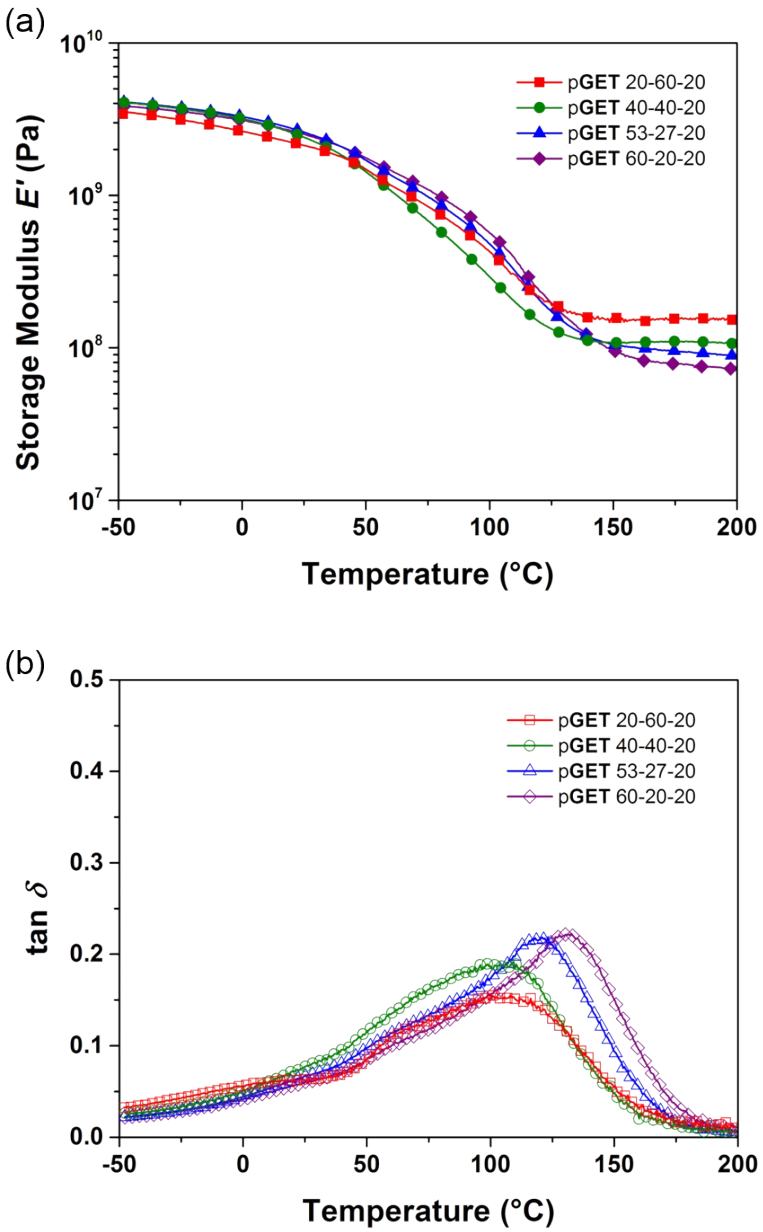

Figure S22. DMA of p**GET** terpolymers at different **G:E** ratios (a) storage modulus *E'* and (b) dissipation peak tan δ as a function of temperature.

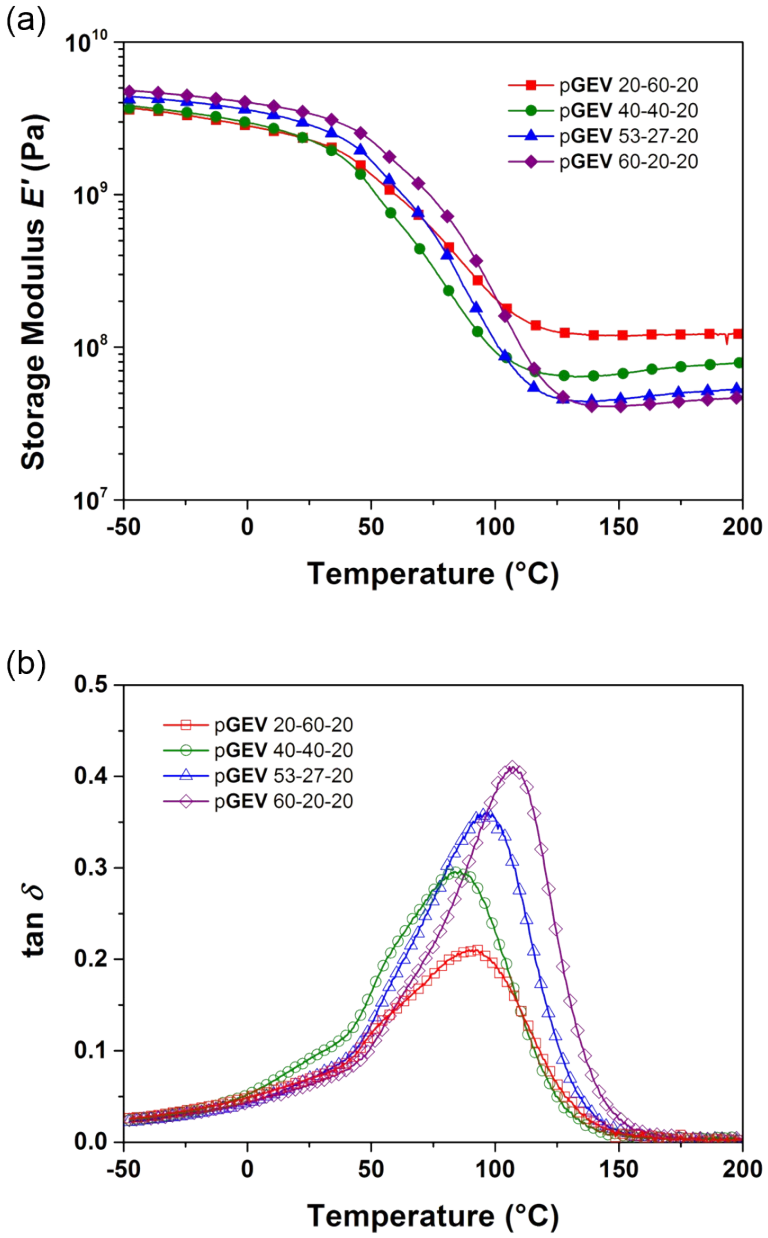

Figure S23. DMA of p**GEV** terpolymers at different **G:E** ratios (a) storage modulus *E'* and (b) dissipation peak tan δ as a function of temperature.

Table S1. Composition profiles of binary and ternary formulations of (meth)acrylates.

Formulation	Function-ality	G		E	
		Mol%	Wt %	Mol%	Wt %
GE 25-75	1.75	25	9.4	75	90.6
GE 50-50	1.5	50	23.7	50	76.3
GE 75-25	1.25	75	48.2	25	51.8

Formulation	Function-ality	G		E		T	
		Mol%	Wt %	Mol%	Wt %	Mol%	Wt %
GET 20-60-20	2	20	8.0	60	77.8	20	14.2
GET 40-40-20	1.8	40	19.6	40	63.1	20	17.3
GET 53-27-20	1.67	53	30.3	27	49.6	20	20.1
GET 60-20-20	1.6	60	37.6	20	40.3	20	22.1

Formulation	Function-ality	G		E		V	
		Mol%	Wt %	Mol%	Wt %	Mol%	Wt %
GEV 20-60-20	1.8	20	8.2	60	79.4	20	12.4
GEV 40-40-20	1.6	40	20.1	40	64.7	20	15.2
GEV 53-27-20	1.47	53	31.1	27	51.1	20	17.8
GEV 60-20-20	1.4	60	38.8	20	41.7	20	19.5

Table S2. Dynamic mechanical properties and cross-link densities of all photocured polymers.

Polymer	T_g (°C)	tan δ_{max}	E' at 25 °C (GPa)	E' at T_g+50 °C (MPa)	v_e ($\times 10^3$ mol/m^3)	Mc (kg/mol)
p**E**	45.0	0.31	0.96	62	3.9	0.15
p**GE** 25-75	57.3	0.33	1.38	53	6.8	0.18
p**GE** 50-50	65.4	0.51	1.60	27	5.9	0.36
p**GE** 75-25	79.7	0.85	2.70	14	2.8	0.72
p**GET** 20-60-20	103.2	0.15	2.12	153	14.4	0.07
p**GET** 40-40-20	106.3	0.19	2.39	108	10.1	0.10
p**GET** 53-27-20	120.3	0.22	2.59	96	8.7	0.12
p**GET** 60-20-20	130.9	0.22	2.51	77	6.8	0.15
p**GEV** 20-60-20	92.4	0.21	2.28	120	11.6	0.09
p**GEV** 40-40-20	84.8	0.29	2.28	64	6.3	0.16
p**GEV** 53-27-20	95.8	0.36	2.86	45	4.3	0.23
p**GEV** 60-20-20	107.5	0.41	3.40	42	3.9	0.26